Int. J. Electrochem. Sci., 11 **(2016)** 8697 – 8708, doi: 10.20964/2016.10.29

International Journal of
ELECTROCHEMICAL
SCIENCE
www.electrochemsci.org

The Effect of Commercialized Binders on Silicon Oxide Anode Material for High Capacity Lithium ion Batteries

Haijun Huang[1,2], *Guangshuai Han*[2] , *Jingying Xie*[2,3,*] , *Quansheng Zhang*[1,*]

[1] Department of Chemical Engineering, Shanghai Institute of Technology, Shanghai 200235, China
[2] Shanghai Institute of Space Power Sources, Shanghai 200245, China
[3] Shanghai Power & Energy Storage Battery System Engineering Tech. Co. Ltd., Shanghai 200240, China
[*]E-mail: jyxie@mail.sim.ac.cn, zhangquansheng@sit.edu.cn

Received: 13 July 2016 / *Accepted:* 11 August 2016 / *Published:* 6 September 2016

The lithium insertion/extraction properties of silicon oxide (SiO_x) composite electrode are investigated using polyvinylidene fluoride (PVDF), LA132 (which major copolymerization chain is polyacrylonitrile-polyacrylic acid (PAN-PAA)) and polyacrylic acid (PAA). Electrochemical cycling tests show that SiO_x electrode with conventional binder PVDF results in rapid capacity fading, while aqueous binders LA132 and PAA remarkably improve the cycle performance of SiO_x at a current density of 80 $mA \cdot g^{-1}$. SiO_x electrode with PAA delivers a reversible capacity up to 1090 $mAh \cdot g^{-1}$ after 50 cycles. All of the electrodes after 10 cycles exhibiting a huge expansion of surface morphology, and some crevices are observed in SiO_x-PVDF electrode. Results of Fourier Transform Infrared Spectroscopy (FTIR) and X-ray diffraction (XRD) show that amorphous or little crystalline grain structure and ester-like bonds are the key factors of adhesion property for binders in SiO_x composite electrode. With cycling, impendence of the SiO_x electrodes with different binders is increasing severely. In addition, the differential capacity plots are used to explain the capacity fading mechanism, the kinetics of electrode process of SiO_x are not affected by applying different binders.

Keywords: Lithium ion battery, Si-based, SiO_x, Binder, High capacity anode

1. INTRODUCTION

Lithium ion batteries (LIBs) have been used widely in various electronic devices, such as portable electronic devices, electric vehicles and energy storage equipment. Presently, graphite (theoretical specific capacity 372 $mA \cdot g^{-1}$) is one of most widely used commercial anode material in conventional LIBs, but it hardly meet the demand of anode materials with the progressing and developing of technique [1]. Recently, SiO_x materials, which owe high lithium storage capacity, have

greatly attracted the researchers' attention. With the advantages of abundant resources and low voltage, a great many researches have reported the excellent electrochemical performance of SiO_x, applied in the field of Si-based materials [2-4]. However, SiO_x materials suffer from the huge volume expansion (up to 200 %) during the lithiation/delithiation processes [5]. The electrodes were pulverized and the electrical contact was greatly weakened because of the accumulated stress [6-8], leading to a worse cycle performance [9]. In order to alleviate the inherent nature of SiO_x materials, many effective methods have been carried out [10], such as carbon coating and metal/silicon doping inert matrix composites [11-13], which significantly improved the conductivity of the electrode and alleviate the volume expansion in a certain extent.

The design of material structure was employed to improve the electrochemical properties of Si-based electrode. On the other way, optimum binder was another key factor to effectively improve the electrode cycle performance and maintain integrity of the Si-based electrode [14, 15]. Hochgatterer et al. [16] used two kinds of carboxymethyl cellulose (CMC) with different degrees of hydroxyl substitution as the binder for the Si/C composites to alleviate the volume expansion during cycling. Other studies also focused on mixing CMC with styrene butadiene rubber (SBR), seeking for proper CMC molecular weight and the optimum pH condition, by which the flexibility and the extensibility of electrode were greatly promoted [17-19]. Polyimide (PI) binder was reported being used in Si-based anode because PI with low breaking elongation percentage and high tensile strength suppresses the collapse of the Si electrode [20]. The conductive polymeric binders developed for graphite/nano-Si anode were proved to be an effective binder for composite electrode, a high areal capacity 2.5mAh·cm^{-2} was achieved over 100 cycles without adding any acetylene black (conductive agent) [21]. Nano-Si electrode with Sodium Alginate (SA) [22] as the binder showed that a high specific capacity up to 1200 mAh·g^{-1} after over 1300 cycles. The carboxyl groups of SA were distributed evenly on the polymer chains and this makes Li ions migrate faster and more efficient.

Herein, we report three different types of binder polyvinylidene fluoride (PVDF), LA132 (the copolymerization aqueous dispersion, which major copolymerization chain is PAN-PAA), and polyacrylic acid (PAA) for SiO_x material. The electrochemical performances were systematically investigated and the function mechanism of different binders was studied for SiO_x electrode. By doing this research, we have found the most suitable binder for SiO_x electrodes/materials, which effectively inhibited the anode swelling, and finally optimized the electrochemical performance.

2. EXPERIMENTAL

2.1. Preparation of SiO_x electrodes

All chemicals were commercially pure and without any further purification. PVDF requires volatile and toxic solvents, N-methyl-pyrrolidone (NMP), and it is always applied in most cathodes and partial anodes. Also, some new environment-friendly aqueous binders were reported being applied, such as PAA. In order to investigate the adaptation ability of SiO_x in different binder systems, PVDF (M_w≈900000, Arkema, France), LA132 (New type aqueous binders, Chengou Indigo Power

Sources Co. Ltd., China) and PAA (M_w≈45000, Aladdin, China) were used as binders in this paper. Electrodes were prepared by slurry casting on copper foil, and the slurry was composed by 80 wt% SiO_x powder (ShinEtsu, Japan), 10 wt% binder and 10 wt% conductive carbon black. Then deionized water or NMP, as dispersions, were added in slurries containing LA132/PAA and PVDF respectively, with stirring for 24 h. The electrodes were dried at 80 ºC to remove deionized water or NMP solvent. Then, the electrodes were cut to disks in a diameter of 14 mm for further coin cell assembling, and finally, the electrode were dried at 120 °C in a vacuum oven for 12 h to remove trace water. The electrodes were marked as SiO_x-PVDF, SiO_x-LA132 and SiO_x-PAA, respectively.

2.2. Electrochemical tests

For electrochemical measurement, conventional CR2016 coin cells were assembled in the argon-filled glove box, high-purity lithium disc as the counter and the reference electrode. 1mol·L^{-1} $LiPF_6$ (EC: DMC=1:1 by volume) with 2 wt% vinyl carbonate (VC) was used as electrolyte. Electrochemical cycling tests were performed with Neware cell test system (Shenzhen Neware Co. Ltd.) at current density of 80 mA·g^{-1} or 160 mA·g^{-1} between 0.01 V and 2 V.

Electrochemical Impedance Spectroscopy (EIS) was used to test electrode with different binders after the 1st, 10th, 20th and 50th cycles. The EIS tests were carried out via using PARSTAT2273 electrochemical workstation in a frequency region of 100 KHz to 10 MHz with amplitude of 10 mV.

2.3. Structure and morphology characterization

The XRD patterns of the SiO_x electrodes were investigated via a Shimadzu-6100 advance diffractometer equipped with Cu-Kα radiation at 40 kV. SEM images were captured using a field emission scanning electron microscope (Hitachi, SU8010) operated at an accelerating voltage of 10 kV. The FTIR spectra of KBr sheets were recorded on a FTIR spectrometer (Shimadzu -IRAffinity-1).

3. RESULTS AND DISCUSSION

3.1. FTIR and XRD analysis

Different binders are characterized by FTIR, as shown in Fig.1. Certain functional groups were observed around the same locations compared with results from others' studies. The 1070~1350 cm^{-1} region corresponds to –C–F in PVDF, and this result was also reported by Gupta et al. [23]. The peaks at 2260 cm^{-1} and 1680 cm^{-1} in LA132 can be assigned to –C≡N and carboxyl (–COOH), respectively. PAA shows a complex spectrum with two peaks at 1710 cm^{-1} (corresponding to the –C=O stretching vibration of the carboxyl group) and 2940 cm^{-1} (–O–H), suggesting the appearance of –COOH [24]. While the peak at 1400 cm^{-1} can be assigned to hydroxyl (–O–H).

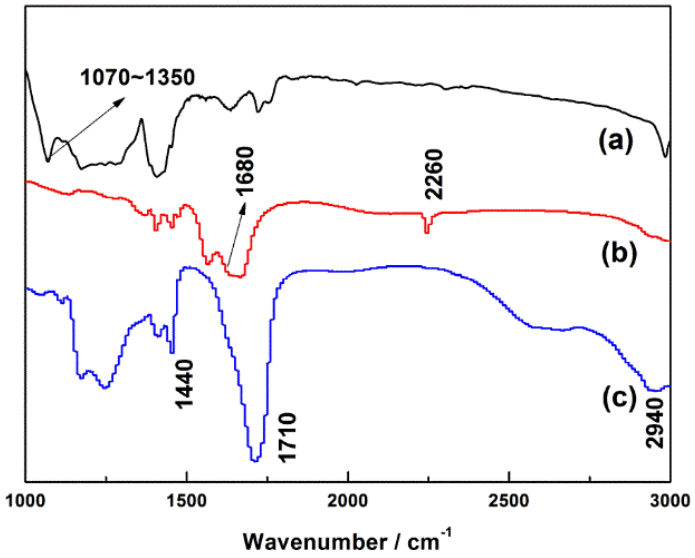

Figure 1. FTIR spectra of the binders (a) PVDF, (b) LA132, (c) PAA

The XRD patterns of different binders are shown in Fig. 2. The morphology of most of the polymers is semi-crystalline, crystallinity can be estimated by comparing the intensity and the width of the curves. From the XRD analysis, PAA just has some dispersion peaks, while notable sharp and narrow diffraction peaks at 18.3º, 20.1º, 26.5º and 17.2º are clearly observed for PVDF and LA132. This indicates PVDF has higher crystallinity and LA132 has partial characteristics of crystallization. The results consist with the former reports [24, 25]. Also, as different manufactures apply different synthetic processes, there are slight differences among their binder products from the characterization results.

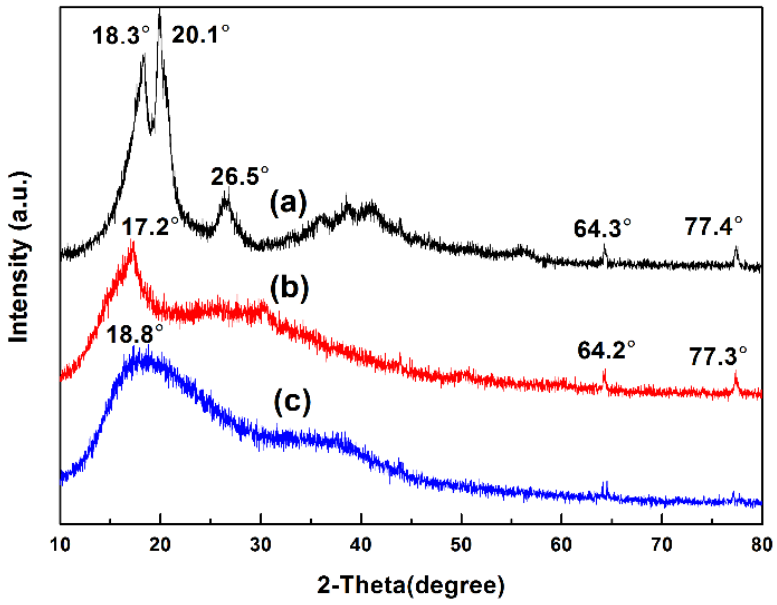

Figure 2. XRD patterns of binders (a) PVDF, (b) LA132, (c) PAA

3.2. Electrochemical Characterization

The cycle performance of the SiO_x electrodes with different binders are shown in Fig.3. The rapid capacity fading of SiO_x-PVDF electrode are observed at current density of 80 $mA \cdot g^{-1}$ and 160 $mA \cdot g^{-1}$ within the first ten cycles. This could be resulted from the overwhelming volume expansion during lithium insertion. PVDF as a thermoplastic material only has an elongation of 20 %~30 % before break [26] and exhibit a strong swelling due to interaction with solvents in the electrolyte [27], therefore, PVDF cannot guarantee the contact between particles and conductive agent. Also, the affected PVDF with weak adhesive property cannot maintain electronic contact between current collector and active materials as well [28]. Compare with SiO_x-PVDF, the capacity of SiO_x-LA132 decay in twenty cycles and the subsequent decay trend gradually slow down with further cycling test moving on. For both tests, SiO_x with PAA binder has the best performance; the capacity still maintain at 1090 $mAh \cdot g^{-1}$ under 160 $mA \cdot g^{-1}$ current density after 50 cycles.

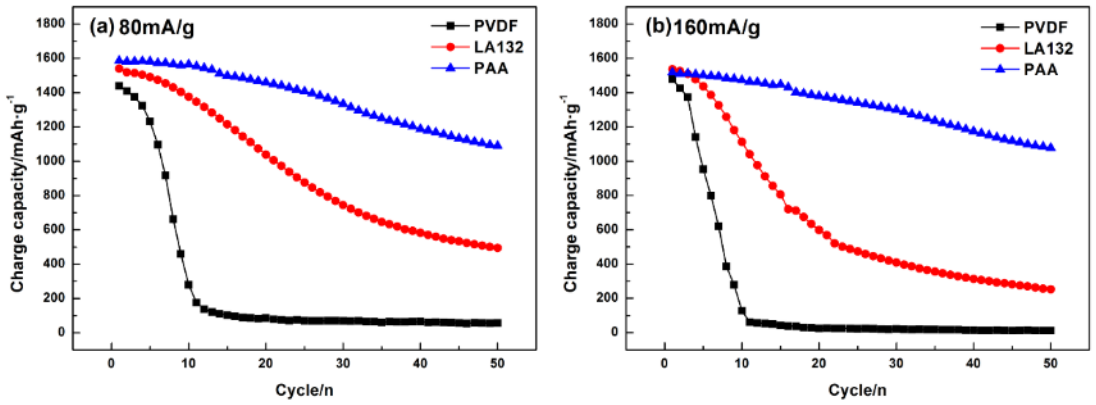

Figure 3. Cycle performance of the SiO_x electrodes with different binders at (a) 80 $mA \cdot g^{-1}$, (b) 160 $mA \cdot g^{-1}$

Fig.4 illustrates the voltage profiles of the SiO_x electrodes with three different binders at a current density of 80 $mA \cdot g^{-1}$ for the initial three cycles. At approximately 0.25 V, a voltage plateau is observed clearly for SiO_x-PAA, suggesting that lithiation process corresponds to the formation of lithium oxide (Li_2O), lithium silicate and silicon [9]. However, SiO_x-PVDF and SiO_x-LA132 show unobvious voltage plateau and constant voltage at first cycle because of the high polarization.

In order to further investigate the influence of different binders on electrode kinetics of SiO_x materials, differential capacity plots are applied to analysis the reason of degradation. Fig.5 shows the dQ/dV plots for the electrodes composed of different binders of the first three cycles. Two anodic peaks at 0.34 V and 0.45~0.47 V are clearly shown in the three samples at the 1st cycle. These peaks typically correspond to delithiation process because of the transformation of amorphous Li_ySi to noncrystalline Si [29], indicating that the use of different binders cannot affect the intrinsic quality of the delithiation process of SiO_x. From Fig.5 (a) and (c), the capacity of SiO_x-PVDF has a significant loss in the first three cycles, while the dQ/dV curves for the other two binders are similar to each other.

The irreversible capacity can be attributed to the following issues: (a) a little of lithium ion was consumed during the irreversible formation of the solid electrolyte interphase (SEI) layer on the electrode surface, which will be proved by EIS analysis in high frequency region; (b) some of lithium ion was trapped in the electrode with the formation of Li_2O, also, the partial inactivating lithium ions do not extract because Li_xSi particle losing connect from the conductive network; (c) the large volume expansion had a significant impact on the conductivity of electrons, thus, the resistance of electrode increased to a great extent, which induced obstacle for lithiation/delithiation process [28]. In addition, the process of delithiation is slower with increasing stress of PVDF.

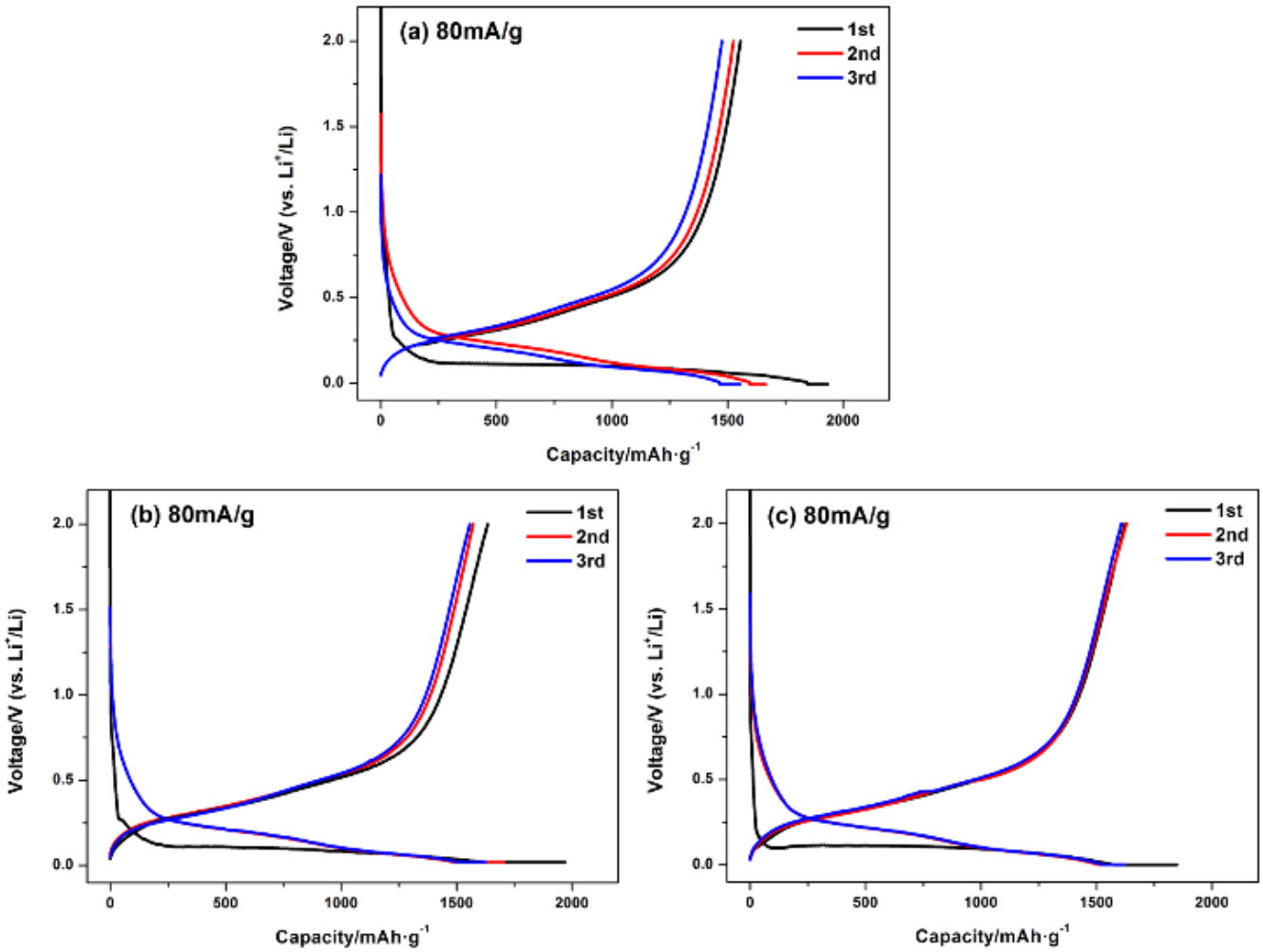

Figure 4. Charge/discharge curves of the SiO_x composite electrodes with (a) PVDF, (b) LA132, (c) PAA as binder

At current density of 80 $mA \cdot g^{-1}$, the peaks of electrodes with different binders have no shift after three cycles, indicating that low current density contributes to stabilize the kinetics of electrochemical process of materials.

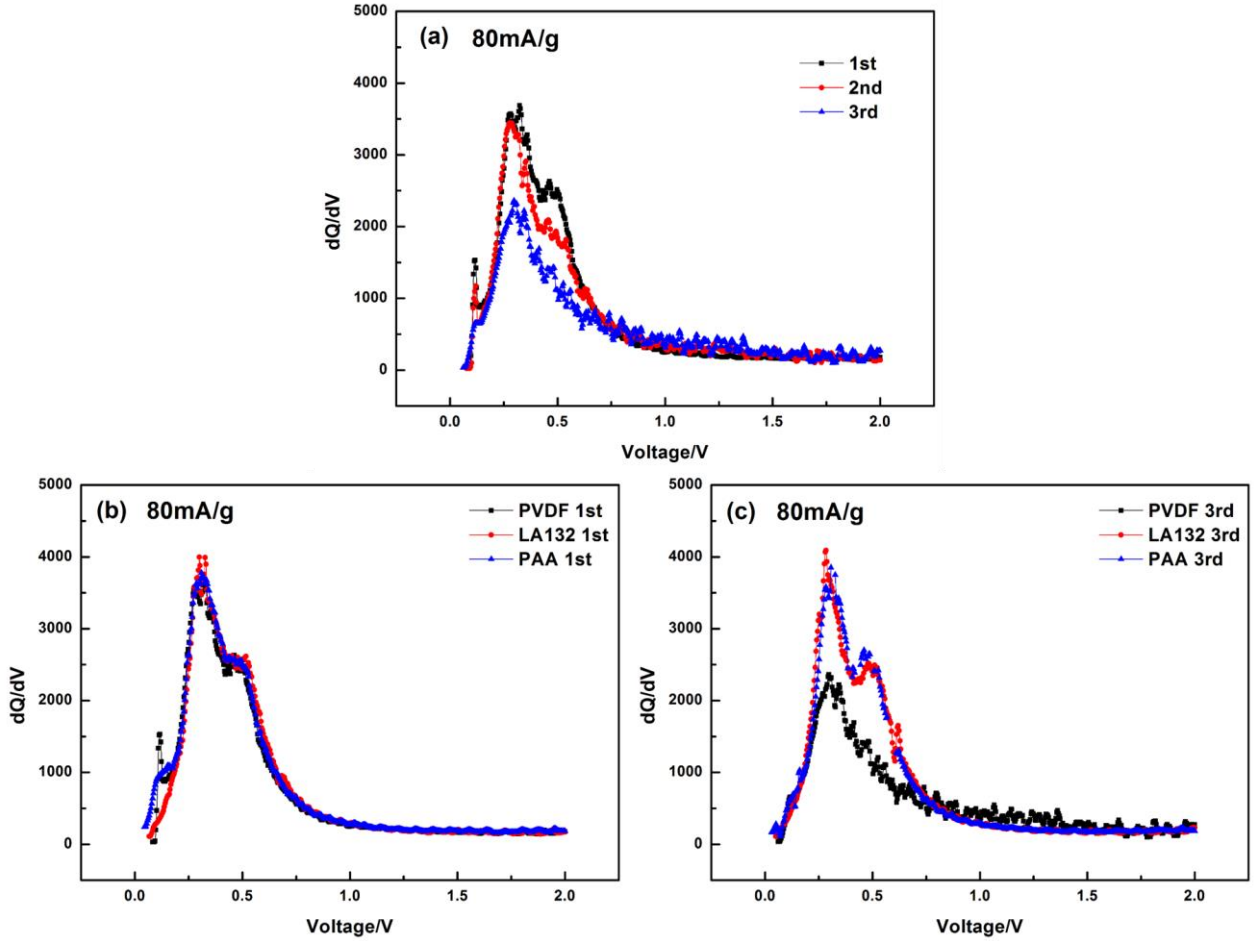

Figure 5. Plots of dQ/dV vs. voltage for (a) SiO_x-PVDF of the initial three cycles; (b) initial cycle with different binders; (c) the 3rd cycle with different binders

The Fig.6 shows the plots of dQ/dV vs. voltage of the SiO_x electrode for the initial 50 cycles. The anodic peaks weaken gradually and vanish after 10th cycle for PVDF. However, from the Fig.6 (b) and (c), the sharp anodic peaks at 0.47 V decrease slowly in fifty cycles. It is probably due to the reaction of unused Li_ySi nanoparticles which are isolated in the deep part of bulk or located close to inactive Li_2O and various lithium silicates [30]. In the first lithiation process, the electrodes are constituted of mixed phase because of the formation of Li_2O, various lithium silicates and Li_ySi. The disordered mixture influence the delithiation process of Li_ySi, so some of Li_ySi lost the ability of lithiation/delithiation. The sharp anodic peaks become stable at around 0.47 V after 20th cycles. With the increasing volume expansion of SiO_x, electrical contact between the active material and the current collector get worse. The reversibility of partial Li_ySi is deteriorated, subsequently it becomes inactive Si-Li alloys. Thus, the delithiation peak at 0.34 V disappears, and only the one at 0.47 V remains. So the process of delithiation in dQ/dV vs. voltage is becoming one main peak.

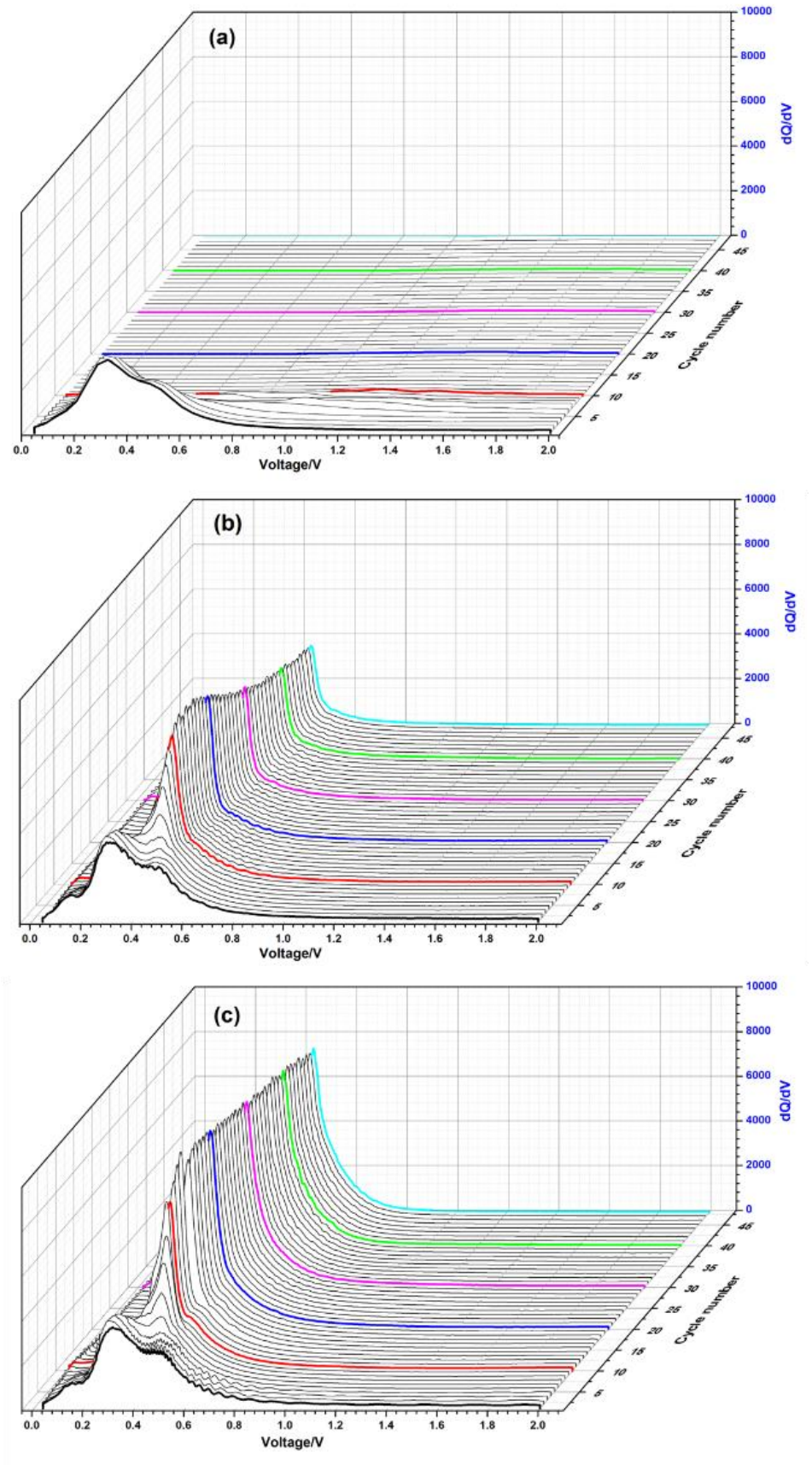

Figure 6. Plots of dQ/dV vs. voltage of the initial 50 cycles at the current of 80 $mA \cdot g^{-1}$: (a) SiO_x-PVDF, (b) SiO_x-LA132, (c) SiO_x-PAA

Fig.7 shows EIS analysis of SiO_x-PVDF, SiO_x-LA132, SiO_x-PAA electrodes at 0.01 V (vs. Li/Li^+), collected after the 1st, 10th, 20th and 50th cycles. The Interface Resistance (R_f) is attributed to the electrode and the electrolyte in the high frequency region. Further instruction, in the intermediate frequency dominated of EIS is regard as Charge Transfer Resistance (R_{ct}) [31]. From the data of EIS, the R_f increases gradually with cycling [32], a behavior that in good agreement with previously reported impedance spectra of silicon-based materials, especially in the electrode with PVDF, which has higher resistance than SiO_x-LA132 and SiO_x-PAA. This result match well with the decay trend of cycle performance. According to the results of the initial 50 cycles, the surface of SiO_x-PVDF electrode and the adhesion of PVDF could be affected, and therefore weakened the conductivity of electrons and lithium ions. The resistance of SiO_x-PVDF increased severely after the 10th cycle, it may be caused by peeling the active material from current collect due to the poor adhesion.

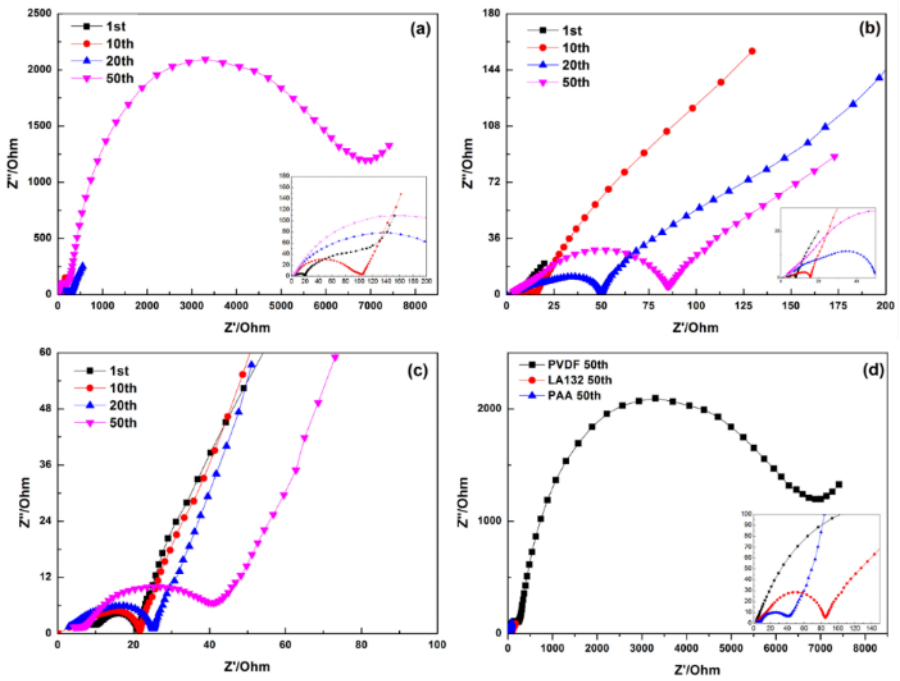

Figure 7. EIS of the SiO_x electrodes with different binders after different cycles: (a) PVDF; (b) LA132; (c) PAA and (d) three binders at 50th charge

Due to changing of the electrochemical properties of partial electrodes after 10 discharge cycles, all of the electrodes are analyzed by SEM to characterize the surface morphology (Fig.8). From the initial electrode morphology, SiO_x particles are irregular and the conductive agent is distributed around the particles uniformly. However, after ten lithium insertion/extraction cycles, the electrode changed. It is obvious that the porosity decreased largely because of significant expansion among the active materials. Some cracks and destructions on the surface can be clearly observed in the SiO_x-PVDF sample in Fig.8 (a2). While, the rest SEM images (b2) and (c2) just show a certain extent expansion and the surface integrity of electrode still remains. The strength, ductility and toughness of the polymer are affected by the portion of microcrystalline and amorphous regions, and this explains

why LA132 and PAA are stronger than high crystallinity PVDF (Fig.2) [25]. Therefore, the adhesion of PVDF is weaker under the large expansibility of SiO_x electrode than LA132 and PAA. These phenomena can be assigned to the lower bonding force of PVDF, which cannot sustain the stress comes from the expansion of SiO_x, and thus the integrity of the electrode is destroyed [28]. Also, compare to PVDF, LA132 and PAA have some effective functional groups like –COOH, which helps to enhance the strength among the particles. Silanol groups (Si–OH) are detected in the SiO_x electrodes that can be explained by the reactions of carboxyl groups and the surface oxygen [33], which yielded a stable surfaces structure containing strong hydrogen bonds [34]. So, the cycle performance of SiO_x has been improved by the stable surface electrode network.

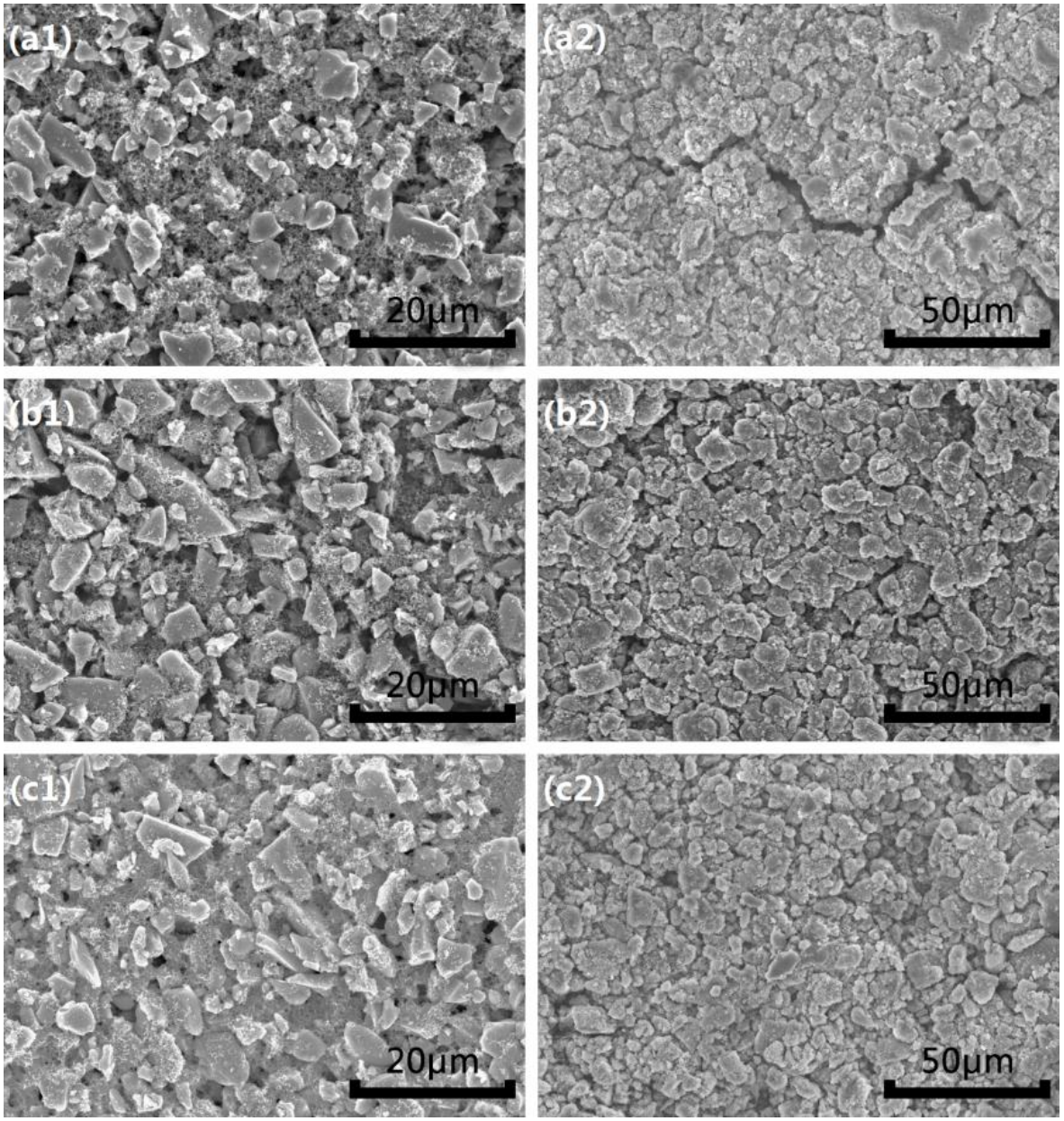

Figure 8. SEM images of the SiO_x electrode before (left) and after (right) 10 discharge cycles (a1), (a2) PVDF; (b1), (b2) LA132; (c1), (c2) PAA

4. CONCLUSIONS

The electrochemical performances of SiO_x materials are systematically investigated with three commercial binders (PVDF, LA132 and PAA). The cycle property is significantly improved by employing LA132 and PAA compare with conventional PVDF binder. SiO_x-PAA still delivers 1090 $mAh \cdot g^{-1}$ after 50 cycles. However, PVDF cannot alleviate rapid capacity decay in initial ten cycles at current density of 80 $mA \cdot g^{-1}$and 160 $mA \cdot g^{-1}$. The degree of crystallization of the binder affects the adhesion and strength of polymer. The low adhesion property of PVDF cannot support large volume expansion of SiO_x because of its high crystallinity. With increasing of cycles, the integrity of the electrode get worse gradually, and R_f rise several times along with lithium inserted/extracted. The presence of the carboxyl groups in PAA and LA132 play an important role to alleviate the volume expansion of the SiO_x material. The results of dQ/dV vs. voltage for SiO_x electrode prove that using different types of binder material for the SiO_x material does not affect the electrode kinetics. And the structural characteristics of the binder itself have a major impact on the electrochemical properties of both the binder material and the battery. Therefore, appropriate binder is critical to improve the cycle life and energy density of high specific energy silicon-based anode.

ACKNOWLEDGEMENTS
The project was supported by the Shanghai Science and Technology Development Fund (15DZ2282000).

References

1. J.R. Dahn, T. Zheng, Y.H. Liu, J.S. *Xue, Sci*. 270 (1995) 590.
2. C.M. Park, J.H. Kim, H. Kim, H.J. Sohn, *Chem. Soc. Rev*. 39 (2010) 3115.
3. M.N. Obrovac, L. Christensen, *Electrochem. Solid-State Lett.* 7 (2004) A93.
4. M.T. McDowell, S.W. Lee, W.D. Nix, Y. Cui, *Adv. Mater*. 25 (2013) 4966.
5. L.Y. Beaulieu, K.W. Eberman, R.L. Turner, L.J. Krause, J.R. Dahn, *Electrochem. Solid-State Lett*. 4 (2001) A137.
6. J.H. Ryu, J.W. Kim, Y.E. Sung, S.M. Oh, *Electrochem. Solid-State Lett*. 7(2004) A306.
7. A. Guerfi, P. Charest, M. Dontigny, J. Trottier, M. Lagacé, P. Hovington, A. Vijh, K. Zaghib, *J. Power Sources* 196 (2011) 5667.
8. Q. Si, K. Hanai, T. Ichikawa, M.B. Phillipps, A. Hirano, N. Imanishi, O. Yamamoto, Y. Takeda, *J. Power Sources* 196 (2011) 9774.
9. J.H. Kim, C.M. Park, H. Kim, Y.J. Kim, H.J. Sohn, *J. Electroanal. Chem*. 661 (2011) 245.
10. X.L. Yang，Z.Y. Wen，L.L Zhang，M. You, *J. Alloys Compd*. 464 (2008) 265.
11. M. Yamada, A. Ueda, K. Matsumoto, T. Ohzuku, *J. Electrochem. Soc*. 158(2011) A417.
12. X.J. Feng, J. Yang, Q.W. Lu, J.L. Wang, Y.N. Nuli. *Phys. Chem. Chem. Phys*. 15 (2013) 14420.
13. M. Miyachi, H. Yamamoto, H. Kawai, *J. Electrochem. Soc*. 154 (2007) A376.
14. H. Zhao, Y.B. Fu, M. Li, Z. Jia, X.Y. Song, Z.H. Chen, J. Lu, K. Amine, G. Liu, *ACS Appl. Mater. Interfaces.* 8(2016) 13373.
15. J. Lopez, Z. Chen, C. Wang, S.C. Andrews, Y. Cui, Z.N. Bao, *ACS Appl. Mater. Interfaces*. 8(2016) 2318.
16. N.S. Hochgatterer, M.R. Schweiger, S. Koller, P.R. Raimann, T. Wöhrle, C. Wurm, M. Winter, *Electrochem. Solid-State Lett*. 11(2008) A76.

17. W.R. Liu, M.H. Yang, H.C. Wu, S.M. Chiao, N.L. Wu, *Electrochem. Solid-State Lett*. 8 (2005) A100.
18. B. Lestriez, S. Bahri, I. Sandu, L. Roué, D. Guyomard, *Electrochem. Commun*. 9 (2007) 2801.
19. J.S. Bridel, T. Azaïs, M. Morcrette, J.M. Tarascon, D. Larcher, *Chem. Mater.* 22 (2010) 1229.
20. S. Uchida, M. Mihashi, M. Yamagata, M. Ishikawa, *J. Power Sources*, 273(2015) 118.
21. H. Zhao, A. Du, M. Ling, V. Battaglia, G. Liu, *Electrochem. Acta*, 209(2016) 159.
22. I. Kovalenko, B. Zdyrko, A. Magasinski, B. Hertzberg, Z. Milicev, R. Burtovyy, I. Luzinov, G. Yushin, *Sci.* 334 (2011) 75.
23. A. K. Gupta, R. Bajpai, J. M. Keller, *J. Polym. Res.* 15 (2008) 275.
24. A. B. D. Osamah, J. Jobin, A. A. H. Mamdouh, *Starch-Stärke* 67 (2015) 1061.
25. A. K.Gupta, R. Bajpai, J. M. Keller, *J. Mater. Sci.* 41 (2006) 5857.
26. J. Li, R. B. Lewis, J. R. Dahn, *Electrochem. Solid-State Lett*. 10 (2007) A17.
27. J.Yang, Y. Takeda, N. Imanishi, T. Ichikawa, O. Yamamoto, *J. Power Sources* 79 (1999) 220.
28. J. Li, L. Christensen, M.N. Obrovac, K.C. Hewitt, J.R. Dahn, *J. Electrochem. Soc*. 155 (2008) A234.
29. H. Takazawa, K. Iwamoto, S. Ito, H. Yoshizawa, *J. Power Sources* 244 (2013) 149.
30. D.T. Nguyen, C.C. Neuyen, J.S. Kim, J.Y. Kim, S.W. Song, *ACS Appl. Mater. Interfaces*. 5 (2013) 11234.
31. R. Ruffo, S. S. Hong, C. K. Chan, R. A. Huggins, Y. Cui, *J. Phys. Chem. C* 113 (2009) 11390.
32. X. L. Chen, K. Gerasopoulos, J. C. Guo, A. Brown, C. S. Wang, R. Ghodssi, J. N. Culver, *Adv. Funct. Mater*. 21 (2011) 380.
33. L. T. Zhuravlev, *Colloids Surf.* A, 173 (2000) 1.
34. A. Magasinski, B. Zdyrko, I. Kovalenko, B. Hertzberg, R. Burtovyy, C. F. Huebner, T F. Fuller, I. Luzinov, G. Yushin, *ACS Appl. Mater. Interfaces*. 2 (2010) 3004.